Support information

Theoretical investigation on the catalytic mechanisms of oxygen reduction and carbon monoxide oxidation on MnNx system

Mingming Luo,[a] Zhao Liang,[a] Mingwei Chen,[a] Chao Liu,[a,b] * Xiaopeng Qi,[a] Shaik Gouse Peera,[c] Juan Liu,[d] Tongxiang Liang[a,*]

[a] Faculty of Materials Metallurgy and Chemistry, Jiangxi University of Science and Technology, Ganzhou 341000, China

[b] State Key Laboratory of Metastable Materials Science and Technology, Yanshan University, Qinhuangdao 066004, China

[c] Department of Environmental Science and Engineering, Keimyung University, Daegu 42601, Republic of South Korea

[d] Department of Mining and Materials Engineering, McGill University, Montreal, QC H3A0C5, Canada

* Corresponding Authors.

E-mail address: liuchao198967@126.com (Chao Liu) and liang_tx@126.com (Tongxiang Liang).

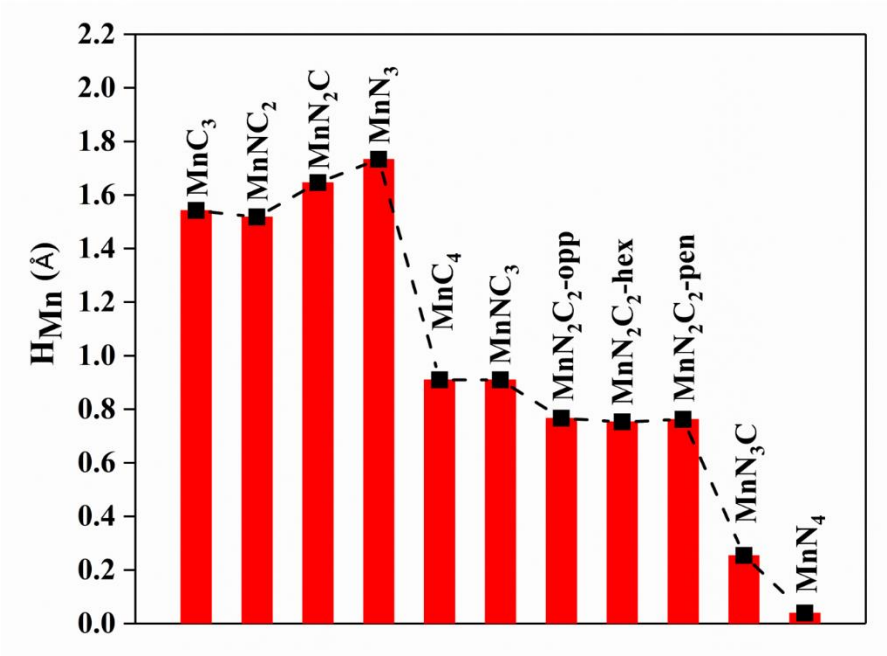

Fig. S1. The measured height of the Mn atom with respect to the graphene basal plane.

	Electrophilic	Nucleophilic		Electrophilic	Nucleophilic
MnC_3	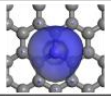	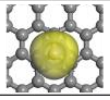	$MnNC_2$	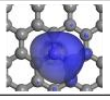	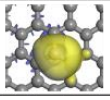
MnN_2C	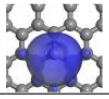	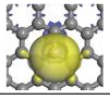	MnN_3	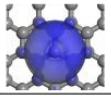	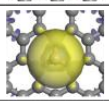
MnC_4	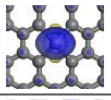	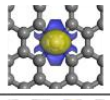	$MnNC_3$	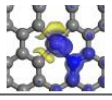	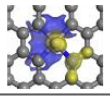
MnN_2C_2-opp	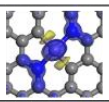	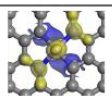	MnN_2C_2-hex	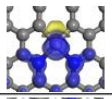	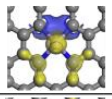
MnN_2C_2-pen	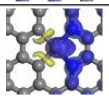	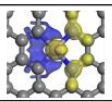	MnN_3C	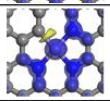	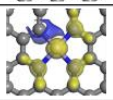
MnN_4	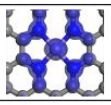	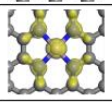			

Fig. S2. The Fukui function of MnN_x, the isosurface value is 4 e/Å^3.

Table S1. Optimized models of different MnN_x configurations and their corresponding ideal *OOH, *O and *OH adsorption configurations.

	Pristine	*O	*OH	*OOH

MnC_3	Top	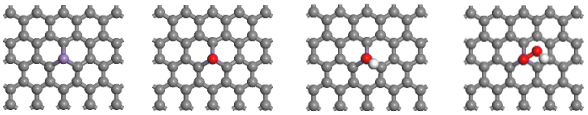			
	Side	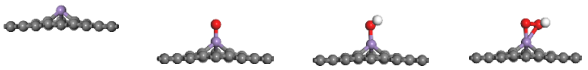			
$MnNC_2$	Top	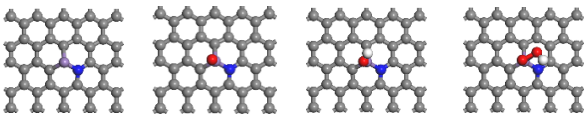			
	Side	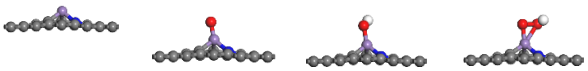			
MnN_2C	Top	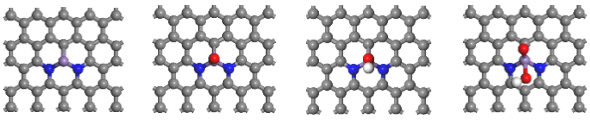			
	Side	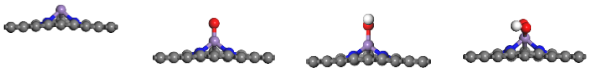			
MnN_3	Top	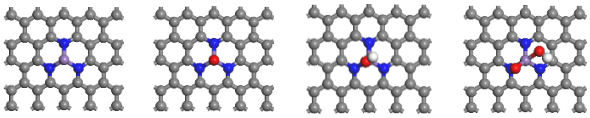			
	Side	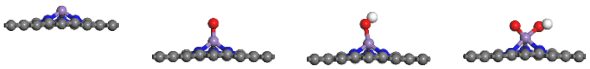			
MnC_4	Top	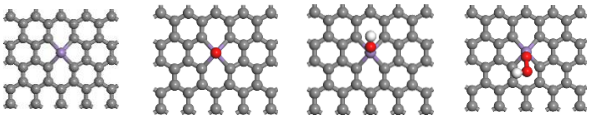			
	Side	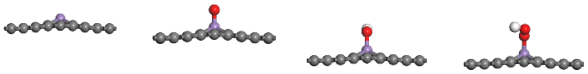			
$MnNC_3$	Top	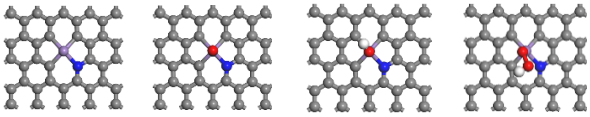			
	Side	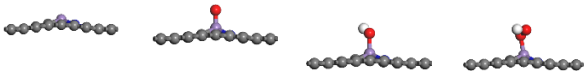			
MnN_2C_2-opp	Top	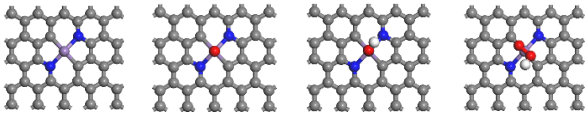			
	Side	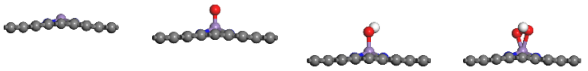			
MnN_2C_2-hex	Top	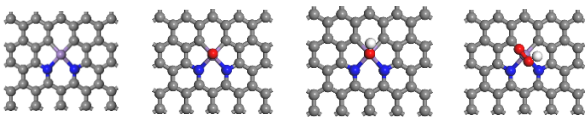			
	Side	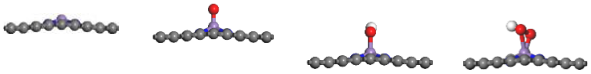			
MnN_2C_2-pen	Top	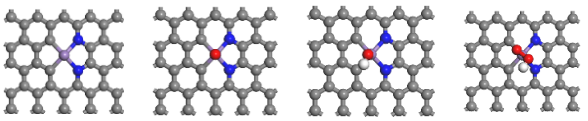			
	Side	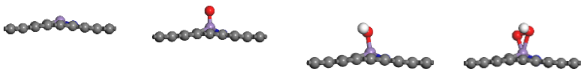			
MnN_3C	Top	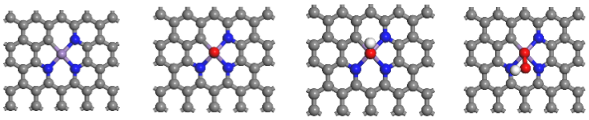			

MnN_4	Side	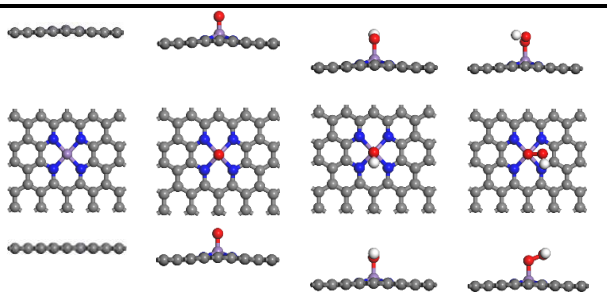
	Top	
	Side	

Table S2. Adsorption free energy (ΔG_{ads}, eV) of ORR intermediates (OOH, OH and O) in MnN_x

Structures	G*OOH	G*O	G*OH
MnC_3	1.877	-0.060	-1.317
$MnNC_2$	1.633	-0.846	-1.347
MnN_2C	-	-1.062	-1.281
MnN_3	-	-1.280	-1.277
MnC_4	2.516	-0.464	-0.644
$MnNC_3$	2.660	0.031	-0.426
MnN_2C_2-opp	2.634	0.070	-0.362
MnN_2C_2-hex	2.736	0.237	-0.279
MnN_2C_2-pen	2.634	0.015	-0.211
MnN_3C	2.727	0.367	-0.243
MnN_4	2.996	0.629	0.019

Table S3. Free energy variations (eV) of the ORR pathways for MnN_x structures and their corresponding theoretical overpotentials (V)

Structures	ΔG_1	ΔG_2	ΔG_3	ΔG_4	η
MnC_3	-3.043	-1.938	-1.257	1.317	2.547
$MnNC_2$	-3.287	-2.479	-0.500	1.347	2.577
MnN_2C	-5.539	-0.443	-0.219	1.281	2.511
MnN_3	-5.433	-0.767	0.002	1.277	2.507
MnC_4	-2.404	-2.980	-0.180	0.644	1.874
$MnNC_3$	-2.260	-2.629	-0.457	0.426	1.656
MnN_2C_2-opp	-2.286	-2.564	-0.432	0.362	1.592

MnN_2C_2-hex	-2.184	-2.500	-0.516	0.279	1.509
MnN_2C_2-pen	-2.118	-2.787	-0.227	0.211	1.441
MnN_3C	-2.193	-2.360	-0.610	0.243	1.473
MnN_4	-1.924	-2.367	-0.610	-0.019	1.211

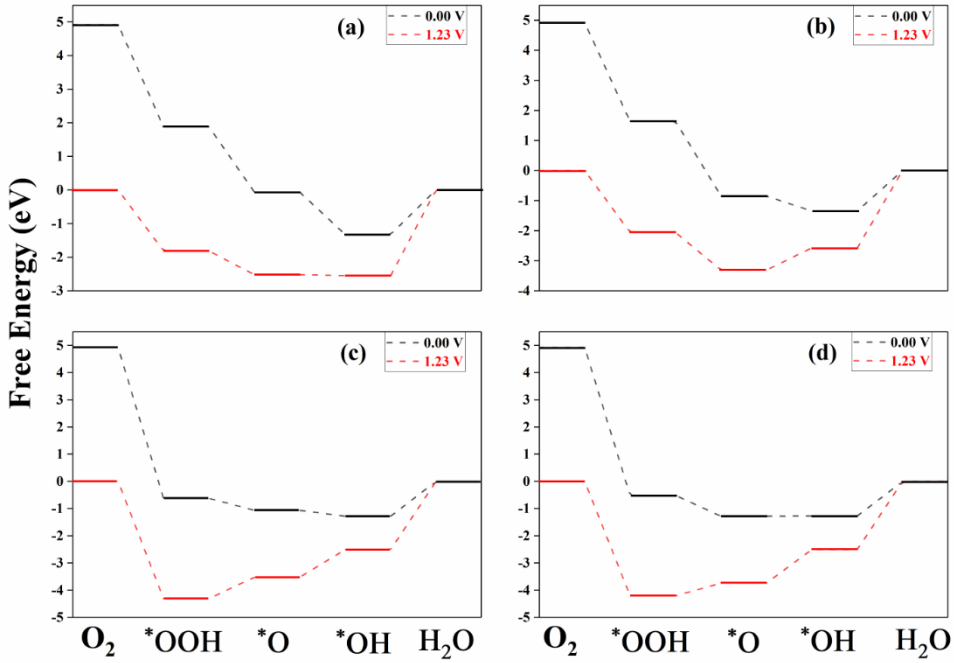

Fig. S3. The free energy (eV) diagrams of ORR pathways on three-coordinate structures. (a) MnC_3, (b) $MnNC_2$, (c) MnN_2C, (d) MnN_3.

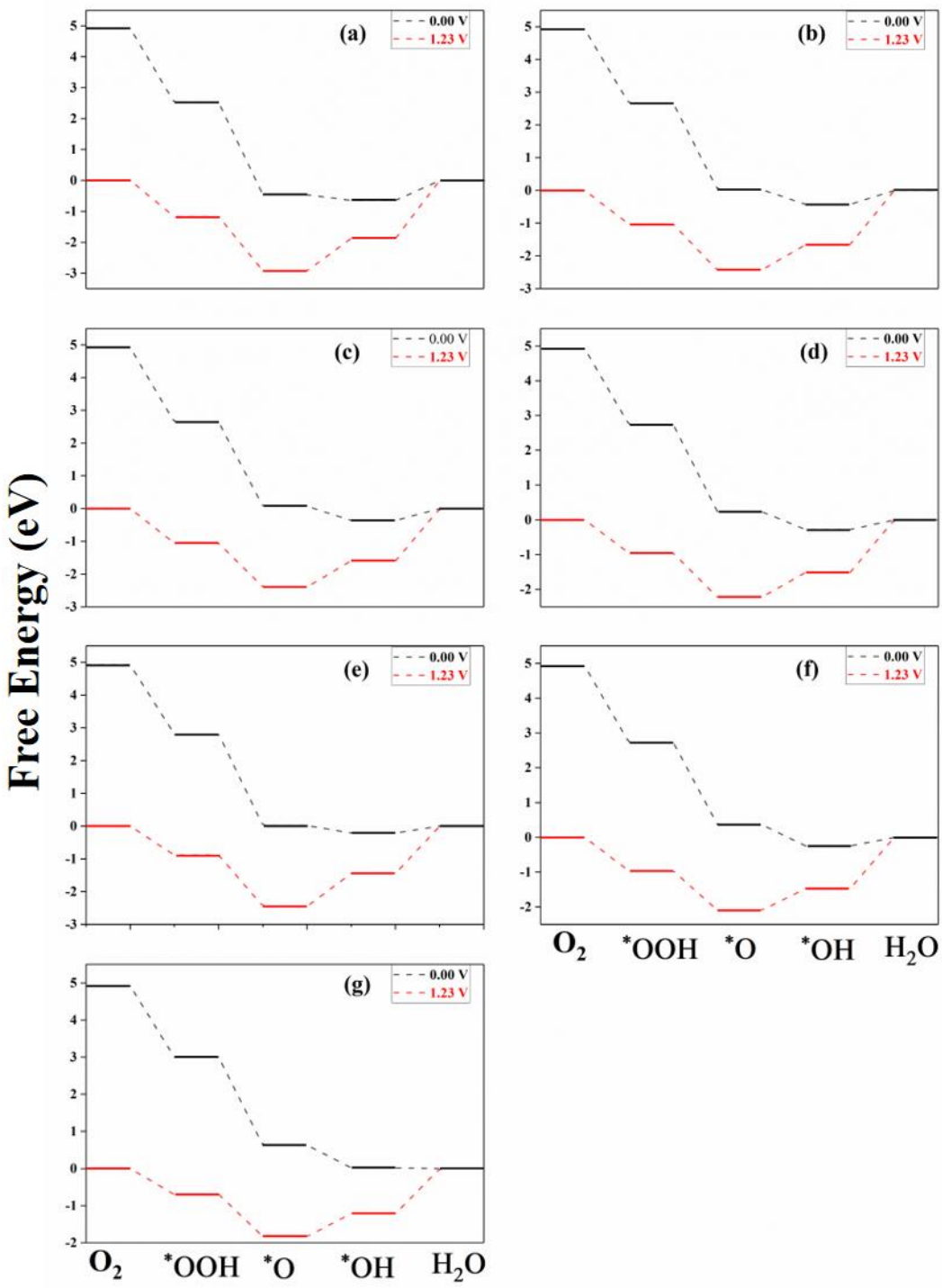

Fig. S4. The free energy diagrams of ORR pathways on four-coordinate structures. (a) MnC_4, (b) $MnNC_3$, (c) MnN_2C_2-opp, (d) MnN_2C_2-hex, (e) MnN_2C_2-pen, (f) MnN_3C, (g) MnN_4.

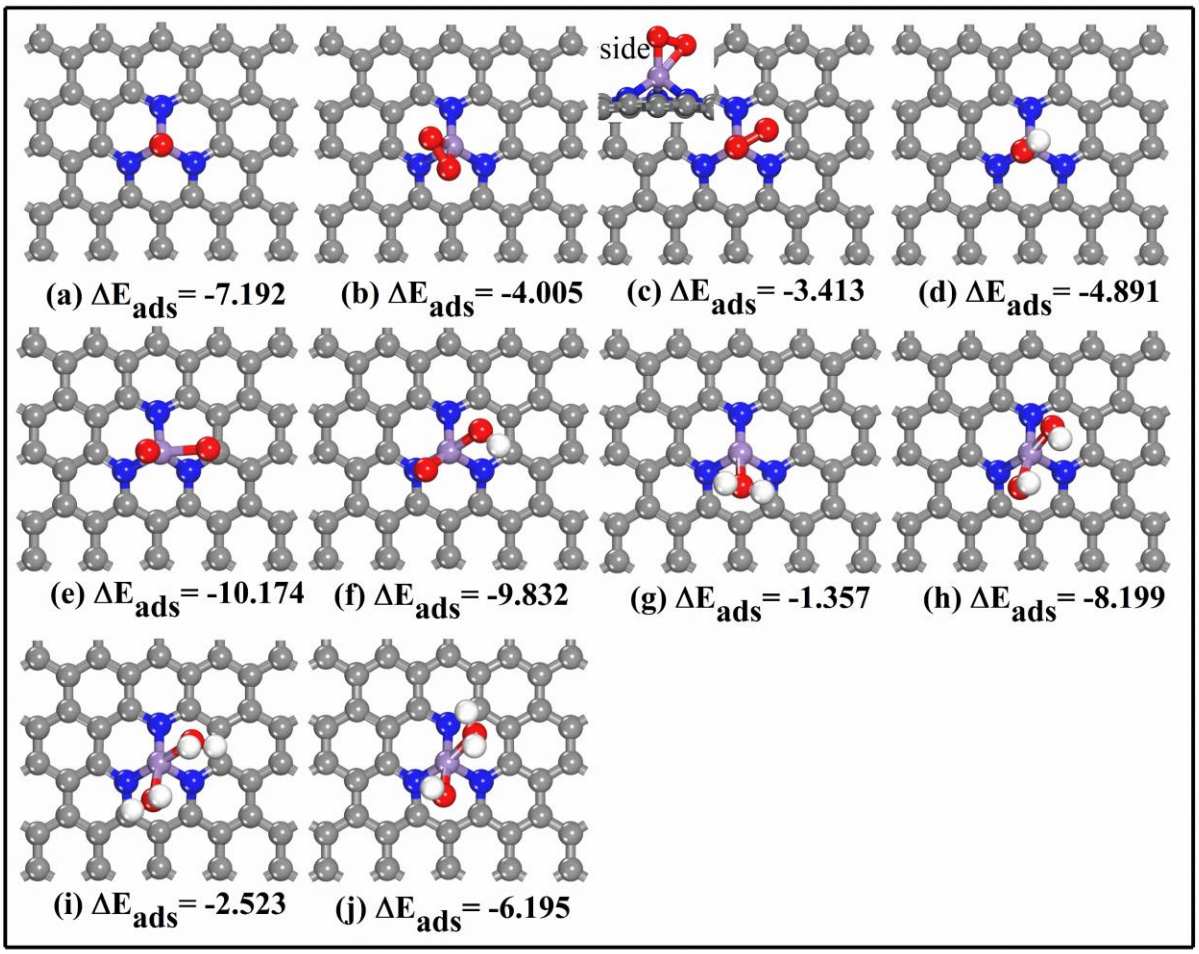

Fig. S5. The most stable adsorption configurations of the ORR intermediates on the MnN_3, ΔE_{ads} is the adsorption energy (eV).

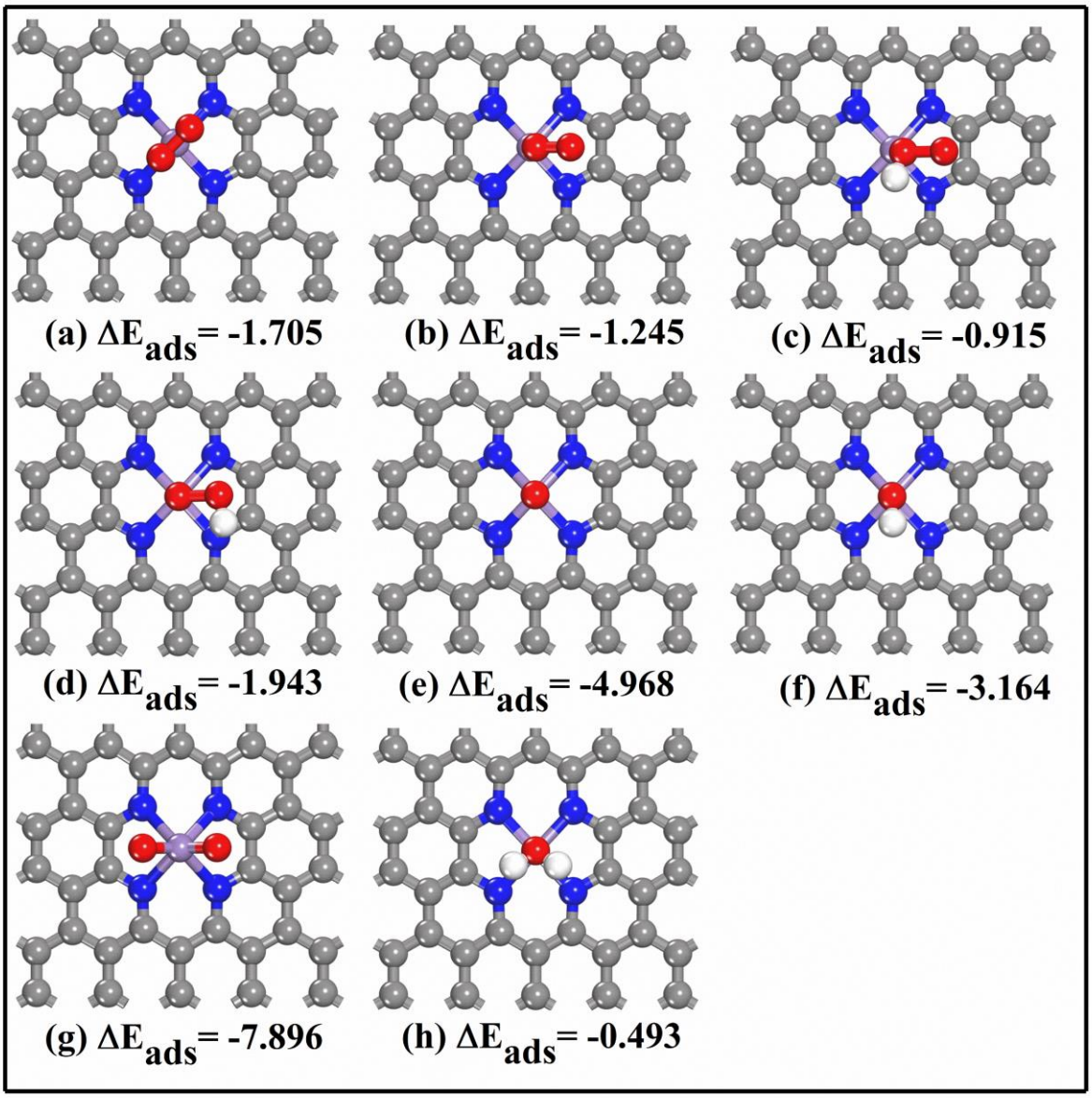

Fig. S6. The most stable adsorption configurations of the ORR intermediates on the MnN_4, ΔE_{ads} is the adsorption energy (eV).

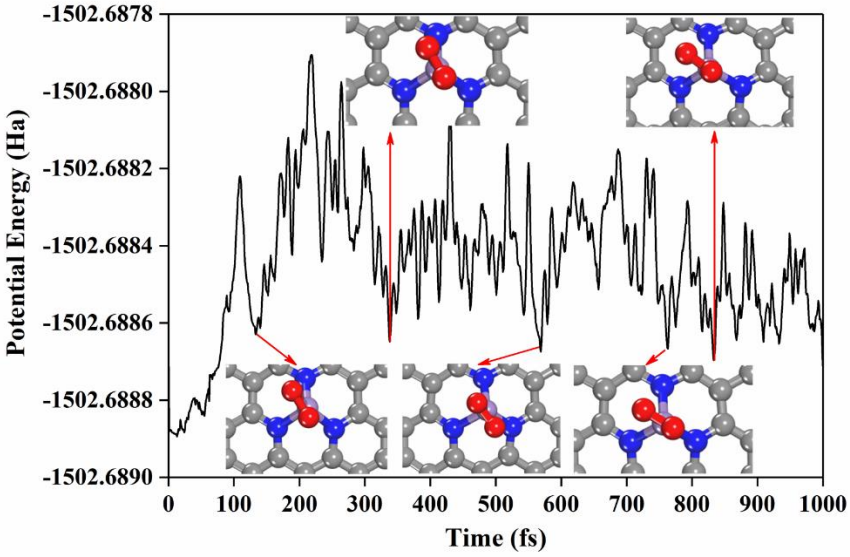

Fig. S7. The structural change of side-O_2[1] comes from the molecular dynamics of 300 K.

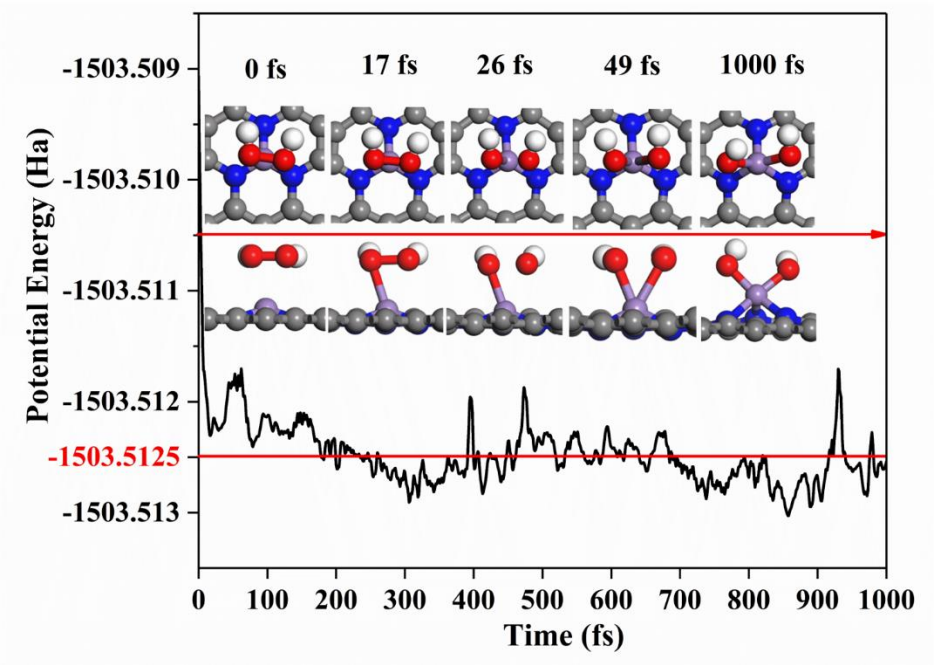

Fig. S8. The structural change of HOOH comes from the molecular dynamics of 300 K.

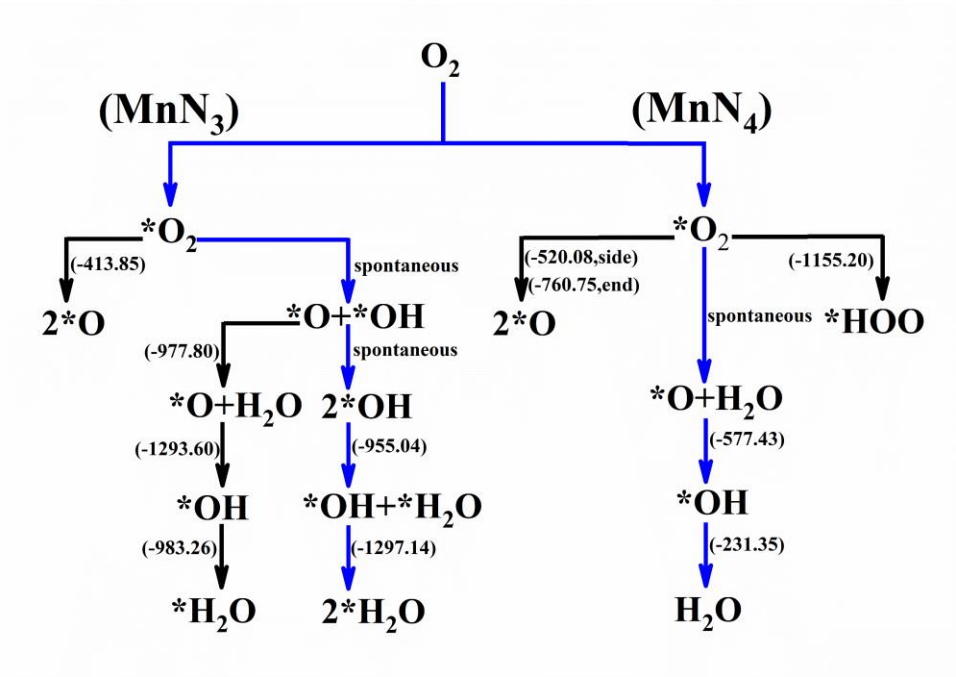

Fig. S9. The reaction pathway for ORR on MnN_3 and MnN_4, the best path is marked with blue arrow. The numbers in parenthesis are imaginary frequencies (cm^{-1}) of transition states. * denotes that the ORR intermediate is adsorbed on the catalyst surface.

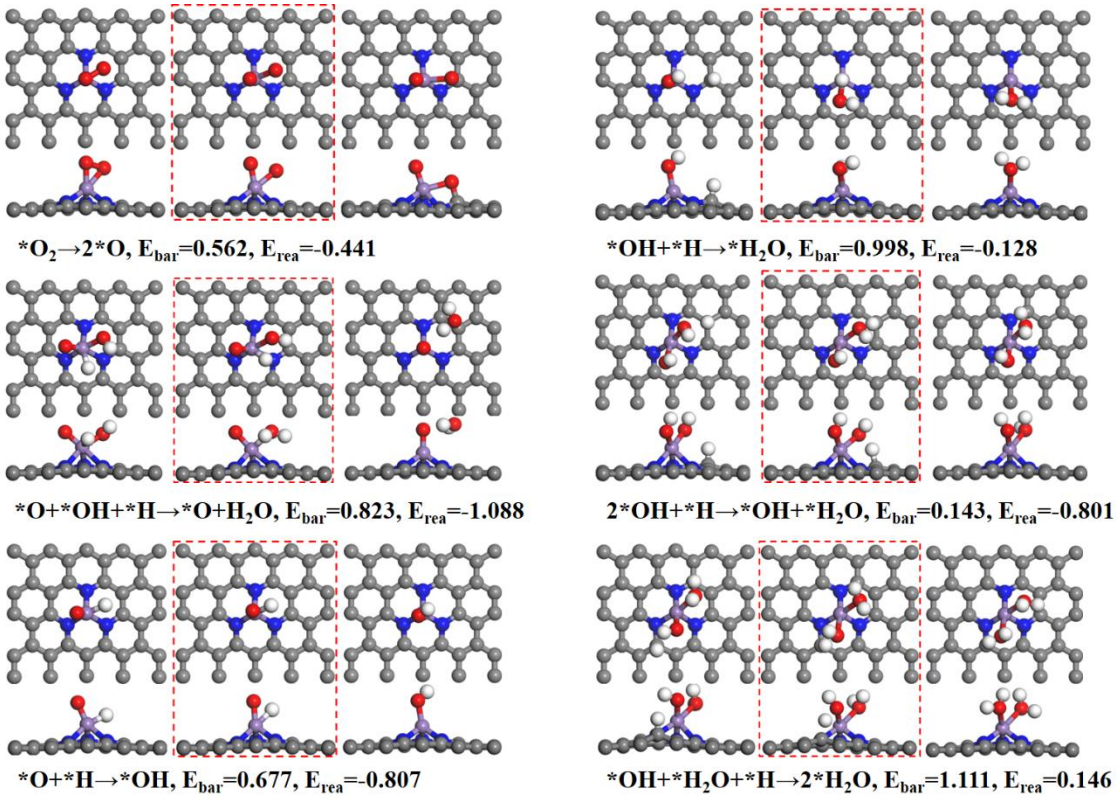

Fig. S10. Structures for the most favorable ORR pathway on MnN_3. From left to right in each row: initial state, transition state and final state, the transition state structure is selected with dashed frame. E_{bar} represents reaction barrier (eV) and E_{rea} represents reaction energy (eV).

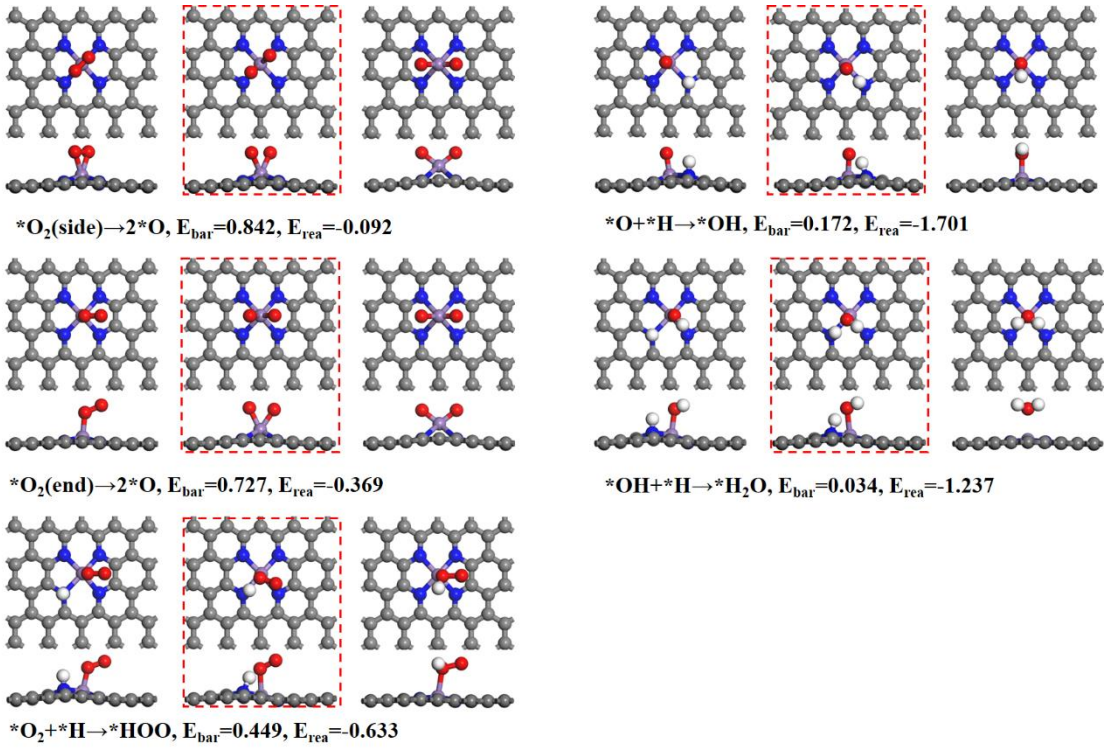

Fig. S11. Structures for the most favorable ORR pathway on MnN_4. From left to right in each row: initial state, transition state and final state, the transition state structure is selected with dashed frame. E_{bar} represents reaction barrier (eV) and E_{rea} represents reaction energy (eV).

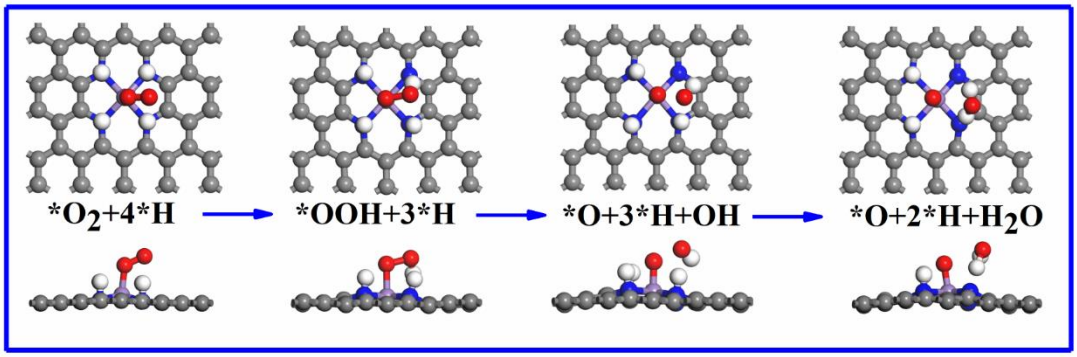

Fig. S12. The structural change of O_2 comes from the molecular dynamics of 300 K.

Table S4. The adsorption energies (eV) of O_2, CO and O_2 + CO on MnN_X.

Models	$\Delta E_{ads}(CO)$	$\Delta E_{ads}(O_2)$	$\Delta E_{ads}(O_2+CO)$
MnC_3	-1.506	-2.324	-2.749
$MnNC_2$	-1.864	-2.987	-3.393
MnN_2C	-1.899	-3.457	-4.103
MnN_3	-1.912	-3.182	-4.344
MnC_4	-1.205	-2.048	-2.339
$MnNC_3$	-1.331	-1.972	-2.276
MnN_2C_2-Hex	-1.448	-1.778	-2.490
MnN_2C_2-Opp	-1.318	-1.975	-2.283
MnN_2C_2-Pen	-1.424	-1.655	-2.327
MnN_3C	-1.460	-1.758	-2.135
MnN_4	-1.389	-1.449	-1.341

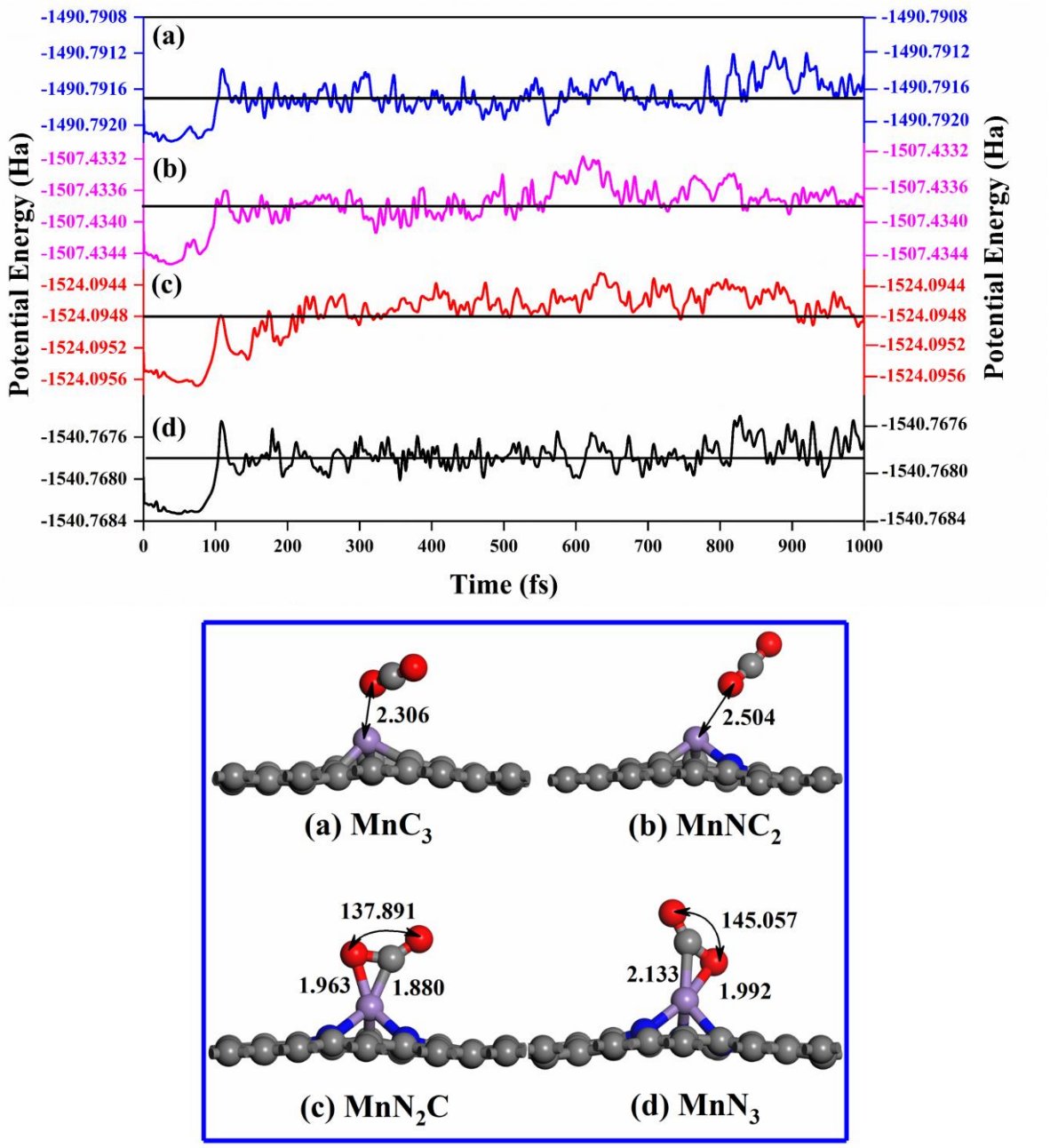

Fig. S13. The molecular dynamics simulation of (a) MnC_3, (b) $MnNC_2$, (c) MnN_2C, (d) MnN_3 adsorbing CO_2 at 300 K.

Table S5. Imaginary frequencies (cm^{-1}) information of CO oxidation along various mechanisms on MnN_4.

	TS1	TS2
ER	-596.97	-392.29
$*O_2 \rightarrow 2*O$	-593.22	
$*O_2+CO \rightarrow *O+CO_2$	-567.8	
NER	-268.92	-154.22
LH	-328.09	-394.08

*O+CO→CO_2	-615.65	
TER	-46.13	-653.94